

Atom Holography at Light Structures

Stefan Bernet, Roland Abfalterer, Claudia Keller, Markus K. Oberthaler, Jörg Schmiedmayer and Anton Zeilinger

Institut für Experimentalphysik, Universität Innsbruck, Technikerstraße 25, A-6020 Innsbruck, Austria

We present diffraction experiments where the roles of light and material are inverted with respect to usual holography. Atomic matter waves are diffracted at grating structures composed of standing light waves. In contrast to material holograms, our light gratings can be manipulated during the passage of an atomic matter wave, resulting in new diffraction features. We demonstrate similarities and differences between material and light holograms.

Journal of Imaging Science and Technology 41: 324–331 (1997)

Introduction

The interaction of waves with periodic media provides a plethora of beautiful coherent wave phenomena^{1,2} that are particularly striking for de Broglie waves of massive particles. Atoms interacting with standing light waves are a model system to study these phenomena.^{3,4} Recently, atom wave diffraction of a computer-generated material hologram was demonstrated.⁵

In a typical holographic experiment, a light wave is diffracted at a hologram consisting of a material grating structure. In the following, we will call such an experiment conventional holography. In contrast, we investigate in our experiments the complementary case of atomic matter wave diffraction at standing light fields. This kind (or prestage) of light-controlled atomic holography might become very interesting for producing nanostructures in atomic lithography applications as well as in fundamental research as an additional test of static and time-dependent quantum mechanics.

In conventional holography, the features of the diffraction process such as the diffraction efficiency and the angular and wavelength selectivity are determined by the recording geometry (reflection or transmission holograms), the use of thin (Raman-Nath case) or volume holograms (Bragg or van Laue diffraction), and the recording mechanism (absorption holograms or refractive index holograms).

Interestingly, all these features are preserved or are similar to those in matter-wave holography. The analogies are even present in very detailed diffraction effects such as the *anomalous transmission* of waves through an absorptive grating structure (the Borrmann effect) or the phase relations between atoms scattered at absorptive and refractive index structures leading to a violation of Friedel's law, as we will show later.

However, there are some additional features in our case of matter-wave diffraction at light gratings. These effects

arise if time-dependent manipulation of a light crystal is performed during the passage of a slow atom. Parameters of our standing light grating, such as intensity, frequency, phase, and polarization can easily be modulated on a time scale needed by the atom to transverse the light field. The complementary case using material gratings and light waves is almost impossible to achieve because of both material restrictions and the high photon velocity. Thus, in some sense, matter-wave diffraction can be seen as a generalization of photon diffraction, as it preserves the diffraction features of static diffraction experiments and enables some new observations using time-dependent manipulations.

Basics

A standing light wave couples with an atomic matter wave, if the light frequency is close to an electronic transition of the atom. If the light is resonant, the interaction results in diffusion or absorption (corresponding to a transition to another electronic state) of the atom and an effectively absorptive grating results. Off-resonant light acts as a refractive index grating for the atomic matter wave. As is the case with conventional holography, the interaction of the atomic matter waves with the light field can be attributed to a complex refractive index, consisting of an imaginary part that describes the absorption of atoms, and a real part corresponding to the real index of refraction.

In the case of our two-level argon atom with an additional decay channel of the excited state to a third noninteracting state, the interaction between the light field and the atom leads to a complex refractive index proportional to⁶

$$1 - n \approx \frac{U}{2E_{kin}} = \frac{d^2 E^2}{\Delta + i\gamma/2} / 2\hbar E_{kin}. \quad (1)$$

Here U is the light potential seen by the atom, E is the electric field connected to the light, d is the dipole matrix element of the transition, Δ represents the difference between the driving light frequency and the eigenfrequency of the transition, γ is the loss rate from the excited level to the noninteracting state, and E_{kin} is the kinetic energy of the atom.

Original manuscript received January 26, 1997.

©1997, IS&T—The Society for Imaging Science and Technology

Note that the shape of this complex index of refraction is identical to the complex index of refraction produced by an absorption center (such as a dye molecule) in a material hologram.

All time-independent diffraction properties of atomic matter waves at a light field described by such complex index of refraction can be treated in full analogy with dynamical diffraction theory of light.^{7,8} In our case the atom is described by a de Broglie wave with wavevector $k_{dB} = mv/\hbar$ and frequency

$$\omega_{dB} = \hbar k_{dB}^2 / 2m$$

(m and v are the mass and the velocity of the atom, respectively). The standing light field produces a periodic modulation of the complex refractive index that diffracts atomic matter waves in the same way as a periodic material structure diffracts photons. Particularly, the diffraction theories developed for light diffraction⁸ at thin (Raman-Nath) or thick (Bragg) gratings or absorptive or refractive index gratings can be directly mapped to the matter waves.

As in the case of conventional holography, the coherence properties of the incident wave are important. To obtain diffraction, the transverse spatial coherence length of an atom has to be larger than the grating constant. This can be achieved by collimating the atomic beam. As in the case of a light beam, a small transverse momentum uncertainty Δp_{trans} results in a large transverse coherence length l_{coh} of the beam $l_{\text{coh}} \sim \Delta p_{\text{trans}}/\hbar$. In our actual case, we achieved a transverse coherence length of approximately 5 μm using a set of two narrow slits to confine the atomic beam direction.

The temporal coherence (or longitudinal coherence length) of an atomic beam depends on the velocity distribution of the atoms, which can be transformed to a wavevector distribution. This is similar to the case of the temporal coherence of a light beam, which is also determined by its frequency (or wavevector) bandwidth. Because of the velocity dependence of the de Broglie wavelength, the temporal coherence of an atomic beam can be increased by velocity selection of the atoms, for example, by using a set of beam choppers. The argon atoms of our experiment emerge from a thermal source, resulting in a longitudinal coherence length of only 10^{-11}m . The various spectral components of the atomic beam are scattered at different diffraction angles, depending on the wavelength sensitivity of the diffraction grating.

As compared to historical optical research, one can say that our study of atomic matter-wave diffraction is in an early stage of optical diffraction experiments using diffraction gratings with rather large grating constants and incoherent light sources with spatial coherence obtained by reducing their size.

In the following, we give a brief description of our experimental apparatus and describe our first experiments demonstrating some very basic effects in static and dynamic potentials.

Experimental Setup

Details of the interaction between atom and light field depend on the level scheme of the atom chosen. All our experiments were performed using a beam of metastable argon atoms,⁹ obtained by a dc gas discharge in an argon atmosphere. Metastable ^{40}Ar has a simple but very interesting level scheme. Starting from the $1s_5$ metastable state there is a closed transition ($1s_5 \rightarrow 2p_9$) at 811 nm ($J = 2 \rightarrow J = 3$) and an open transition ($1s_5 \rightarrow 2p_8$) at 801 nm ($J = 2$

$\rightarrow J = 2$) where the decay proceeds with 72% to the argon ground state. The metastable atoms can be easily detected using a channeltron detector (which acts similar to a photomultiplier tube), whereas the ground state Ar atoms remain undetected. Thus, the argon atoms that relax to the ground state are lost to detection and may be considered as absorbed by the complex potential. This offers the interesting possibility of realizing amplitude gratings (absorptive structures) with light fields. Varying the detuning of the 801-nm standing light wave, we can, thus, realize any real, complex, or imaginary sinusoidal potentials for the metastable argon atoms.

Figure 1 shows our experimental setup. Behind the dc gas discharge region, a thermal beam of metastable argon atoms enters a vacuum beamline. Our atomic beam apparatus is designed to resolve the tiny deflection of atoms when diffracted at a standing light wave with a 405 nm ($\lambda_{\text{light}}/2$) period ($\vartheta_{\text{diff}} \approx 32 \mu\text{rad}$ for 800 m/s atoms). The high resolution for transverse deflections is obtained with two separate collimation sections, each of them formed by two narrow slits (typically 5 or 10 μm wide) with a spacing of 1 m. Finally, the fine spatial resolution of the detector is achieved by scanning a small (10- μm) slit in front of the channeltron. We obtain an angular resolution of about 7 μrad FWHM significantly smaller than the deflection angle by the scattering of a single 800-nm-wavelength photon.

Experimentally, the standing light wave is realized using a retro-reflecting mirror ($\lambda/10$ flatness) arranged close to the atomic beam inside the vacuum chamber. The surface of the mirror defines a node of the standing light wave and, hence, the lattice planes of the light crystal parallel to the mirror surface.

Rotating the mirror around a vertical axis results in a change of the incidence angle of the atoms at the light crystal. Measuring the angular dependence (in our experiments with accuracy and reproducibility of $\pm 1 \mu\text{rad}$ using a PZT) of the transmitted or diffracted intensity (a rocking curve) provides an experimentally simple and robust way to study the diffraction processes in the crystal.

The mirror can also be translated in a direction perpendicular to the atomic beam with a resolution of 0.5 μm .

For the standing light waves, the laser beam is expanded with a Keplerian telescope. The expanded beam is transversely limited by an aperture of up to 4 cm diameter in the various experiments.

A laser diode tuned to an electronic ($1s_5 \rightarrow 2p_8$) transition at 801.7 nm provides the light for realization of the absorption crystal. A second laser diode tuned close to another electronic transition ($1s_5 \rightarrow 2p_9$) at 811.8 nm is used to make a phase crystal, as mentioned above.

Atoms in Crystals of Light

First, atomic matter-wave diffraction experiments using detuned light (refractive index gratings) in the thin grating regime were performed.¹⁰ The scattered atoms appeared in a broad range of incidence angles, and the diffraction efficiency was symmetric in conjugated diffraction orders.

Then, Bragg scattering of atoms from thick standing light waves was reported by Ref. 11 and, more recently, by Refs. 12 and 13.

In those studies, well-known phenomena from conventional holography were observed: In contrast to the thin grating diffraction regime, first-order diffraction occurred now only in one diffraction order and under two special symmetric angles of incidence $\pm\theta_B$, where the Bragg angle θ_B is given by the same relation as in conventional holography:

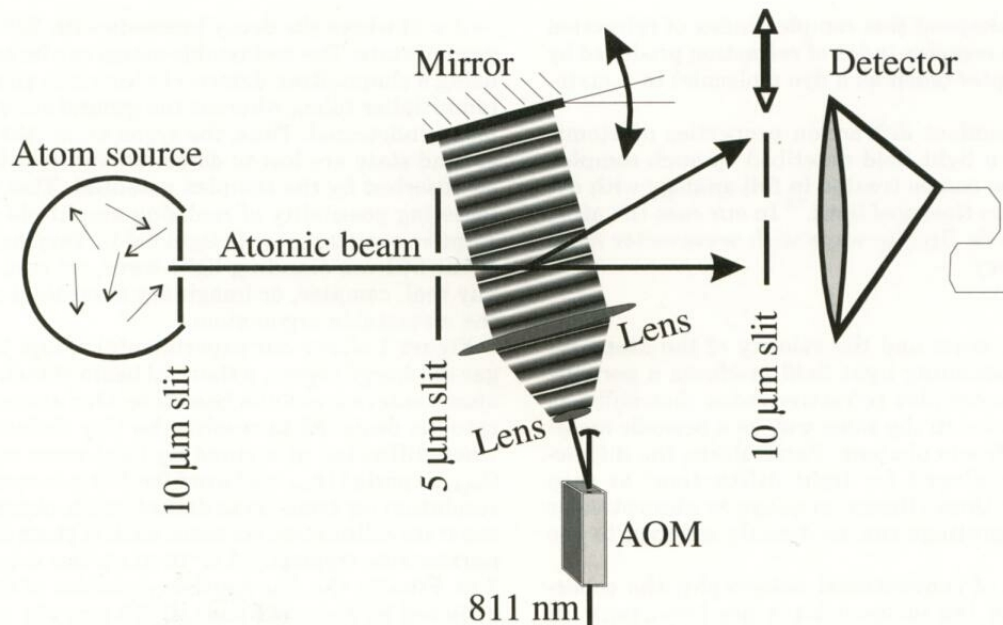


Figure 1. Experimental setup (from Refs. 3 and 4). A collimated thermal beam of metastable argon atoms crosses a standing light wave. Diffracted and transmitted atoms are registered by a channeltron detector. The angle between atomic beam and light wave can be varied by tilting the mirror. The intensity of the laser light can be modulated by an acousto-optic modulator (AOM).

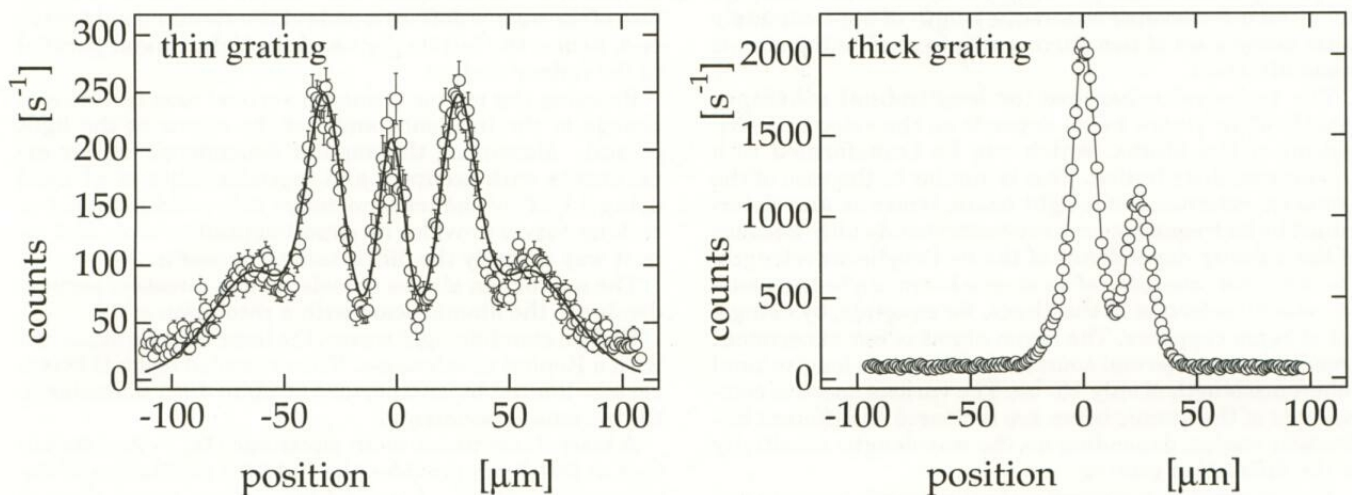


Figure 2. Comparison of matter-wave diffraction at thin and thick off-resonant standing light waves. The atoms are registered as a function of the detection slit position with the setup of Fig. 1. The left plot shows the result for diffraction at a focused (100- μm) standing light wave. The diffraction is symmetric with respect to the central peak of undiffracted atoms, and higher diffraction orders are also populated. The right plot shows the result of the same experiment performed with an extended (thickness: 4 cm) light crystal. Only one single peak of diffracted atoms appears in addition to the central peak of transmitted atoms. The incidence angle in this experiment was exactly the Bragg angle, otherwise no diffracted atoms were observed at all.

$$2d_g \sin(\theta_B) = \lambda_{dB}. \quad (2)$$

Here, d_g is the grating constant of the light intensity grating and λ_{dB} is the de Broglie wavelength of the atom.

Figure 2 shows spatially resolved atomic diffraction experiments at thin and thick light gratings, recorded with the setup of Fig. 1 by scanning the detection slit. As expected, the diffraction at the thin grating is symmetric with respect to the central peak of undiffracted atoms, and higher diffraction orders are populated. But in the Bragg case, the peak of diffracted atoms appears only if the mirror angle is adjusted exactly to the corresponding Bragg

angle. Only one diffraction order is populated at a certain incidence angle. Diffraction to the conjugate order (the other side of the transmitted atoms) is only observed if the mirror angle is adjusted at the symmetric angle with respect to the incident atomic beam.

Increasing the length (or intensity) of the light crystal leads to the well-known Pendellösung phenomenon,^{12,13} where the diffracted intensity oscillates with the length of the Bragg crystal between 0 and 100%. The transition from the thin grating regime to the thick grating regime occurs because of the same condition as in conventional holography. If an atom incident under the Bragg angle

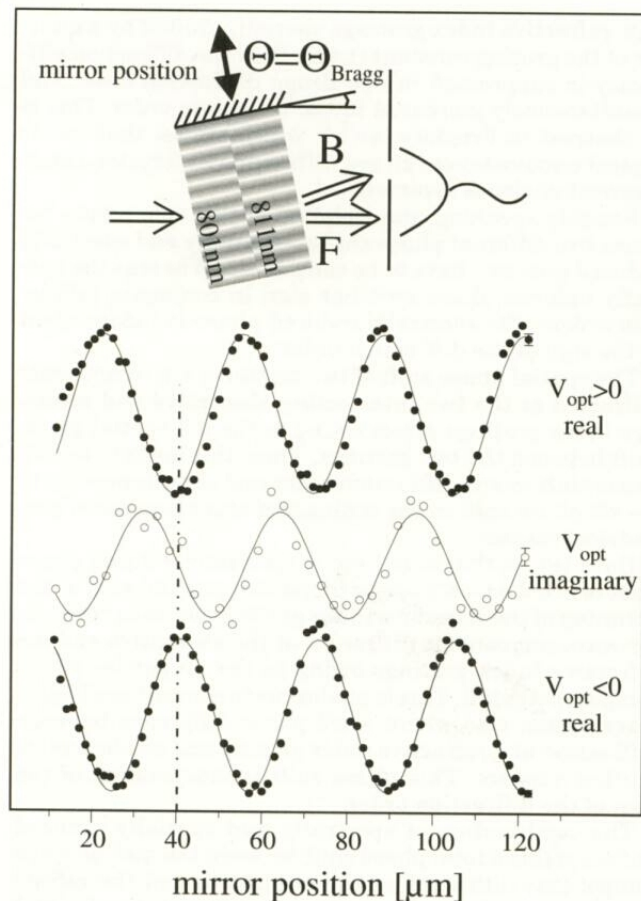


Figure 3. Measurement of the standing atomic wave fields in the light crystal.³ The matter-wave field produced by the absorptive crystal (on-resonant light, middle trace) has its maxima at the nodes of the light intensity planes. If the 801-nm standing wave is detuned off-resonance (refractive index crystal), the standing atomic wave is shifted by $\pi/2$ to the left for blue detuning (positive potential) or to the right for red detuning (negative potential).

crosses more than one grating plane, then the light structure acts as a thick diffraction grating. The relative angular and wavelength selectivity of the light crystal corresponds in the same way as in conventional holography to the inverse number of crossed grating planes.

In the following, we present experiments studying the coherent motion of atoms in crystals made from on- and off-resonant light. The experiments confirm that atoms fulfilling the Bragg condition form a standing matter-wave pattern. As a consequence, we observe anomalous transmission of atoms through resonant light fields and an astonishing symmetry breaking known as violation of Friedel's law. We also demonstrate how Bragg diffraction of atomic matter waves at a time-modulated thick standing light wave can be used to shift the de Broglie frequency of the diffracted atoms coherently. The mechanism is similar to an acousto-optic frequency shifter for photons.

Coherent Atomic Motion in Periodic Light Structures

In our first set of experiments we studied the coherent motion of atoms in crystals made from on- and off-resonant light.³ The basic phenomenon of Bragg scattering of atoms from thick far off-resonant standing light waves has been observed by others.¹¹⁻¹³ More recently, light gratings

were used as beamsplitting mechanisms in atomic matter-wave interferometers, demonstrating impressively the coherence of the diffraction process.^{14,15}

Our experiments directly confirm the validity of coupled wave theory and dynamical diffraction theory as developed for light optics^{7,8} and matter-wave optics.^{2,16,17} There, Bragg diffraction is described as a coherent superposition of two coupled waves within the crystal. The coupled waves should form an atomic density grating with the same periodicity as the diffraction grating propagating through the light crystal. In the case of an absorptive Bragg crystal, the nodes of the atomic wave field should lie on the maxima of the light intensity grating, which means that the atoms emerge on the dark places of the grating. But if the light frequency is detuned to the red or blue side of the atomic transition frequency, the spatial phase of the standing atomic matter wave is assumed to shift by $+\pi/2$ or $-\pi/2$, respectively. In this case, the atoms emerge on one of the flanks of the light intensity grating, depending on the signs of the detuning and the diffraction order. All these phenomena are well known in the dynamical diffraction theory of conventional holography. We now turn to the question of observing the atomic wave fields inside the light crystal.

The coherence and the relative phase of the outgoing beams can be measured by recombining them and observing their interference. Experimentally, we realized this by placing an additional phase Bragg crystal behind the absorptive phase crystal made with 801 nm light (see inset Fig. 3). The new phase crystal was realized with a laser tuned far-off-resonance to the closed transition at 811 nm (red detuned). Because the two standing light waves have different wavelength, the relative phase $\Delta\phi$ between the two crystals varies as a function of the distance Δx from the mirror

$$[\Delta\phi = 2(\vec{k}_1 - \vec{k}_2) \cdot \Delta\vec{x}]$$

resulting in a spatial beating period of 32.4 μm . By moving the mirror, one can translate the two crystals relative to each other and observe the interference as an intensity variation with the beating period in the two outgoing Bragg-diffracted beams.

The data from an experimental study in this two-crystal geometry are shown in Fig. 3. The top curve shows the interference pattern for a far blue detuned light crystal made from the 801-nm laser light, and the bottom curve shows the pattern for the far red detuned crystal. We observed the expected π phase shift that arises when the light shift potential switches sign for red and blue detuning. The curve in the middle was observed for the first crystal exactly on-resonance at 801 nm. First, the interference confirms the coherence of the observed two beams emerging from the first crystal, even on-resonance. Second, we observe the expected phase shift of $\pi/2$ relative to the far off-resonance cases.

In a separate experiment we determined the absolute position of the standing matter-wave pattern at the exit of a far off red detuned 811 nm light crystal by masking it by a thin on-resonant 801 nm amplitude grating. The gold surface of the retroreflecting mirror defined the nodes of the electric fields for both frequencies. Measuring the transmitted intensity as a function of the distance of the atomic beam from the mirror surface allowed us to determine the absolute position of the standing atomic wave field. We found for on-Bragg incidence the maximum of the atomic wave field in the off-resonant light crystal to be located at the steepest gradient of the optical potential, in accordance

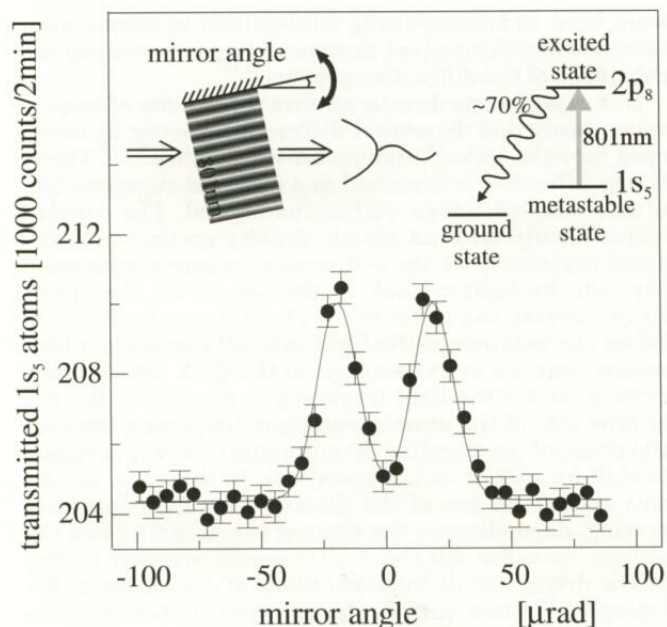


Figure 4. Total intensity of the metastable Ar^* beam as a function of incidence angle after transmission through a standing light wave tuned exactly on resonance of an open transition (see insert).³ The light field can be considered as absorptive for the metastable atoms because the atoms relax to their nondetectable ground state after interaction with a photon. The transmission increases anomalously for Bragg incidence from either side relative to the planes of the standing light field. The solid line is a fit curve using two Gaussians.

with the above description. The position scale in Fig. 3 reflects this measurement.

As just demonstrated, the atomic matter waves in the light crystal behave in full analogy with light waves in conventional periodically modulated refractive index crystals. This should also lead to more detailed analogies with well-known optical diffraction effects. One of them is the anomalous transmission effect discovered for x rays by Borrmann¹⁸ in 1941. We started by investigating the propagation of atoms in an on-resonant standing light wave, equivalent to a purely imaginary periodic potential. We experimentally observed that the total number of atoms transmitted through the standing light wave tuned on-resonance increases if the angle of incidence is the Bragg angle (see Fig. 4). This anomalous transmission of atoms through an absorptive structure has a very clear intuitive interpretation in the coupled wave picture described above. The rate of depopulation of the metastable state is proportional to the overlap between the atomic wave field with the standing light field. It follows that the rate of depopulation is reduced as compared to the average absorption observed for oblique incidence, if the atomic wave field has the same periodicity as the light crystal and lies in the nodes of the light intensity planes. Just this situation arises in the case of Bragg diffraction according to dynamical diffraction theory. If the interaction length is sufficiently long, this results in an increase of transmission on-Bragg as compared to an off-Bragg beam interacting with a light crystal of equal length.

One more astonishing effect, that has also been investigated in conventional holography in frequency selective materials¹⁹ is known as violation of Friedel's law. If a diffraction structure is composed of two identical absorption

and refractive index gratings spatially shifted by a quarter of the grating constant ($\pm\pi/2$), then the diffraction efficiency is suppressed in one Bragg diffraction order and simultaneously increased in the conjugate order. This is in contrast to Friedel's law^{20,21} which states, that under typical circumstances Bragg diffraction at (crystal-) symmetrical angles is symmetrical.

Roughly speaking, the violation of this rule occurs because two different phase shifts—spatially and spectrally induced phases—have to be considered. Whereas the spatially induced phase switches sign in conjugate diffraction orders, the spectrally induced phase is independent of the sign of the diffraction order.

The spatial phase shift of two matter-wave components diffracted at the two intersecting absorptive and refractive index gratings arises owing to the $\pi/2$ spatial phase shift between the two gratings. Thus, this leads to a $+\pi/2$ phase shift in one diffraction order and simultaneously to a $-\pi/2$ phase shift in the conjugated order because of geometrical reasons.

However, at the same time, a spectrally induced phase shift of $+\pi/2$ or $-\pi/2$ arises (depending on the sign of the detuning of the refractive index grating) between the matter-wave components diffracted at the absorptive and the refractive index gratings owing to the properties of the complex potential. This is analogous to conventional light-wave optics, also where a $\pi/2$ phase difference between diffraction at a refractive index grating and an absorptive grating appears. This phase shift is independent of the sign of the diffraction order.

The combination of spectrally and spatially induced phases yields a total phase shift between the matter-wave components diffracted at the absorptive and the refractive index gratings of π in the one diffraction order and simultaneously of 0 in the conjugate order. This consequently leads to destructive and constructive interference in the two diffraction orders, respectively. Effectively, the violation of Friedel's law is thus caused by the different behavior of a spatially induced (by a spatial phase shift) and a spectrally induced (by switching from an absorptive grating to a refractive index grating) phase shift in conjugate diffraction orders.

For an experimental demonstration²² we utilize the fact that two intersecting light crystals can be easily obtained by superposing two light frequencies in one Bragg crystal. One of the frequencies is resonant with the open atomic transition at 801 nm, forming an absorptive crystal, the other frequency is detuned from the closed atomic transition at 811 nm, leading to a refractive index crystal. The two different atomic transitions are chosen to obtain a spatial beating frequency of about $32.4 \mu\text{m}$ between the two gratings (similar to the experiment described above). Thus, by shifting the retroreflection mirror in a direction perpendicular to the atomic beam, we can obtain any spatial phase relation between the two crystals, with a periodicity of $32.4 \mu\text{m}$.

Figure 5 shows the result of an experiment where the diffraction efficiency is compared in the two $+1$ and -1 diffraction orders as a function of the relative spatial phase between the two intersecting light crystals. As expected, maximal asymmetric diffraction is obtained in the case where a spatial phase shift of $+\pi/2$ is applied between the two gratings. This means, that in the experiment a high diffraction efficiency was obtained at a mirror angle corresponding to one of the two symmetric Bragg angles, but almost no diffraction was observed at the corresponding conjugate Bragg angle. In contrast, in the cases of a 0 (or

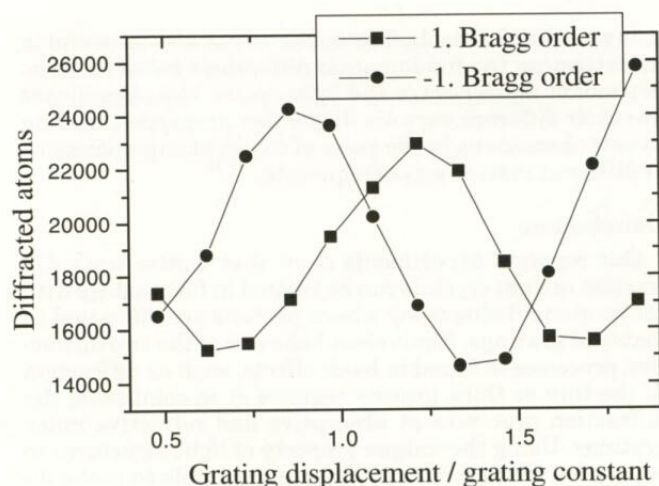


Figure 5. Violation of Friedel's law. The plot shows the diffraction efficiency in the two conjugated first Bragg diffraction orders of a specially designed light crystal. The thick standing light field is composed of two intersecting absorption and refractive index gratings, whose relative phase can be scanned by translating the retroreflection mirror (similar to the inset of Fig. 3, but this time with two superposed light crystals). Experimentally the data have been taken by repetitively adjusting the two symmetric Bragg angles and recording the number of diffracted atoms in the corresponding diffraction orders. The data show that the diffraction efficiency in the two conjugate diffraction orders depends differently on the displacement between the two intersecting gratings. This breakdown of symmetry is a violation of Friedel's law.

π) phase shift between the two crystals, the diffraction efficiency in the two conjugate diffraction orders was symmetric. The asymmetric diffraction efficiency in the cases of the $\pm\pi/2$ phase shifts corresponds to a violation of Friedel's law, which was reported originally for special types of absorptive crystals²¹ and, more recently, for conventional holography in frequency selective materials.¹⁹ The fact that Friedel's law is always fulfilled in any purely absorptive or purely refractive crystal²¹ implies that no pure structure can exist with the same diffraction behavior as our particular combination of absorptive and refractive index gratings. This consequently means that the complete diffraction behavior of an absorptive (a refractive) grating can never be achieved with any specially designed refractive (absorptive) diffraction structure. The scattering processes at the two types of gratings are fundamentally different.

The results obtained so far demonstrate in great detail equivalent behavior of conventional holography and time-independent matter-wave optics in light crystals. However, in the following, we describe experiments that involve time-dependent studies. There, the equivalence of the Schrödinger equation with the optical wave equations (in vacuum) does not hold true any more, and new phenomena may be expected.

Atomic Motion in Time-Dependent Periodic Potential

One advantage of studying the coherent motion of atomic de Broglie waves in light crystals is that the potential can be changed on a time scale much faster than the spatial evolution of the atomic wavefunction. This allows us to study a whole variety of time-dependent phenomena to investigate fundamental predictions of quantum theory.

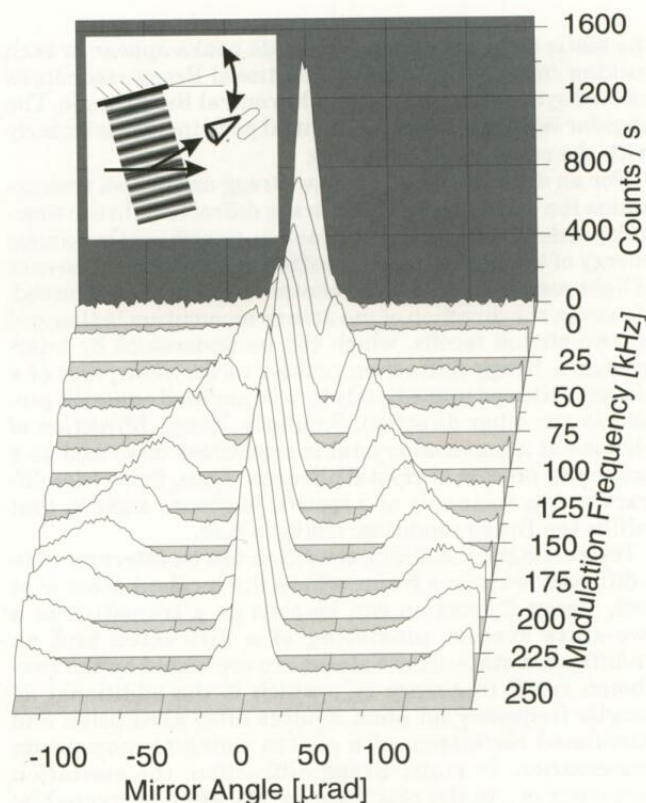


Figure 6. Diffracted atoms as a function of their incidence angle at the amplitude-modulated standing light wave (see inset) at different modulation frequencies.⁴ The detection slit is located such that only diffracted atoms are registered. The top graph of the series shows the result for an unmodulated light crystal. Only one peak of diffracted atoms is observed at the static Bragg angle (center of the plotting region). The next curves show results for intensity modulation frequencies in the range of 25 to 250 kHz in steps of 25 kHz. In contrast to the static case, two pronounced side peaks appear in each curve. They are located symmetrically around the central Bragg angle. Their angular separation from the central peak increases linearly with the modulation frequency. The de Broglie wave frequency of the atoms in the new Bragg peaks is shifted by \pm the modulation frequency.

Experiments using time-dependent interactions were performed within neutron optics and in recent years using cold cesium atoms.²³ In all these experiments the interaction time was much smaller than the modulation period, which is analogous to the Raman-Nath (thin grating) regime in spatial diffraction.

In our experiments, we studied Bragg scattering at a time-dependent potential in a regime where the interaction time is much longer than the typical modulation period. This is obtained by periodically switching the light crystal on and off during the passage of an atom. Obviously, an analogous experiment is almost impossible to perform in conventional holography.

A detailed study of this time-dependent Bragg scattering is shown in Fig. 6. In these experiments, we measure the intensity of the diffracted atoms as a function of the mirror angle (rocking curves), which corresponds to the incidence angle of the atoms at the light crystal. The top graph of the series shows the rocking curve for Bragg scattering off an unmodulated light crystal. Only one peak at the static Bragg angle is observed. The next curves show the same experiment, but with light intensity modulation frequencies in the range of 25 to 250 kHz in steps of 25 kHz. In contrast to

the static case, two pronounced side peaks appear in each rocking curve indicating two additional Bragg resonances located symmetrically around the central Bragg angle. The angular separation from the central peak increases linearly with the modulation frequency.

For an explanation of the new Bragg angles, we first examine the usual case of static Bragg diffraction. In the time-independent case, Bragg diffraction conserves the kinetic energy of the atoms (elastic scattering), similar to the case of light scattering where the photon frequency is conserved. However, the direction of the atomic momentum is changed by two photon recoils, which can be understood by interpreting a Bragg diffraction process as an absorption of a photon, followed immediately by a stimulated emission process in the other direction. Similarly, Bragg diffraction of photons at a material crystal is sometimes described as a scattering process at crystal phonons. Thus, first-order diffraction can occur only at a specific incidence angle θ_B that fulfills the Bragg condition: $\sin(\theta_B) = k_L/k_A$.

Interestingly, the Bragg condition can be interpreted in a different way: In a frame where the incident atom is at rest, Bragg diffraction can be seen as a transition in a two-state system consisting of a diffracted and an undiffracted state. These states are separated by the two-photon recoil frequency ω_{rec} , which is the additional de Broglie frequency an atom acquires after absorption and stimulated reemission of a photon owing to momentum conservation. In static Bragg diffraction, the excitation frequency ω_{rec} in the rest frame of the atom is created by the atomic trajectory crossing the spatially modulated light intensity grating. The time for an atom to pass one light intensity plane at Bragg angle incidence is $\tau = \pi m / \hbar k_L^2$. Thus, in its rest frame the atom experiences a periodic intensity modulation with frequency $\omega_{\text{spat}} = 2\pi / \tau = 2\hbar k_L^2 / m$, which is exactly the two-photon recoil frequency ω_{rec} required for a Bragg transition.

But for an atom incident at an arbitrary detuned angle $\theta = \theta_B + \Delta\theta$, the intensity modulation frequency seen by the atom is $\omega_{\text{spat}} = 2k_L \hbar k_A \tan(\theta_B + \Delta\theta) / m \approx \omega_{\text{rec}} + 2k_L \hbar k_A \Delta\theta / m$. This is not the two-photon recoil frequency required for a Bragg transition, and consequently the atom cannot be diffracted.

However, if the light crystal is additionally intensity modulated with frequency ω_{mod} , the atom experiences a beating of externally (by the external intensity modulation) and internally (by the atomic trajectory crossing the light intensity planes) induced intensity modulations. This results in a sum and a difference frequency $\omega_{\text{beat}} = \omega_{\text{mod}} \pm \omega_{\text{spat}}$ experienced by the atom. Thus, two new resonances appear when ω_{beat} equals the two-photon recoil frequency required for Bragg diffraction. Momentum conservation then requires that in the laboratory frame the frequency of the de Broglie wave diffracted at the temporally modulated intensity grating is shifted by the intensity modulation frequency ω_{mod} . The coherence of the frequency shift has been demonstrated in Ref. 4.

The absolute position of the diffracted peaks in Fig. 6 agrees, within our measurement accuracy, with the positions expected from the above considerations.

As explained above, our device utilizing Bragg diffraction of atoms from a temporally modulated light crystal acts as a frequency shifter for atomic matter waves. Another interpretation of the effect²⁹ suggests that it may be seen as a generalization of an acousto-optic frequency shifter for photons. Such a device might become an important tool in atomic holography applications because it easily manipulates the diffraction properties of atoms without

using mechanical tools. The device might also be useful in investigating the fundamental differences between time-dependent matter-wave and light optics. Most significant are their different vacuum dispersion properties, leading to new phenomena in the cases of coherent superpositions of different matter-wave frequencies.^{30,31}

Conclusion

Our reported experiments show that matter-wave diffraction at light crystals can be treated in full analogy with conventional holography where photons are diffracted at material gratings. Equivalent behavior of the two diffraction processes is found in basic effects, such as diffraction in the thin or thick grating regimes or in comparing the diffraction processes at absorptive and refractive index gratings. Using the unique property of light structures to superpose without interaction, we were able to probe directly the evolution of the atomic intensity distribution within a scattering light crystal. The experiments also verify the coherence of the diffraction processes, which means that a standing light wave acts as a coherent beamsplitter for atomic matter waves. Analogies between matter-wave and conventional holography are found even in very detailed effects such as the anomalous transmission of atoms under Bragg incidence through an absorptive crystal or a violation of Friedel's law resulting from the particular phase relation between diffraction processes at absorptive and refractive index structures.

But differences between matter-wave and conventional holography can be expected in time-dependent experiments. We showed that an intensity modulated light crystal acts as a coherent frequency shifter for atomic matter waves, a generalization of an acousto-optic modulator for photons. Such a device might become very helpful for investigating the exciting similarities and differences between quantum optics of photon and matter waves. Our work opens the way for future experiments that will investigate atomic diffraction at three-dimensional holographic light structures. \blacktriangle

Acknowledgments. This work was supported by the Austrian Science Foundation (FWF) projects S06504 and P10216 and by the European Union Contract No. TMRX-CT96-0002. J. Schmiedmayer is supported by an APART fellowship of the Austrian Academy of Sciences.

References

1. *Atom Interferometry*, P. R. Berman, Ed., Academic Press, 1997.
2. J. M. Cowley, *Diffraction Physics*, North Holland, 1990.
3. M. K. Oberthaler, R. Abfalterer, S. Bernet, J. Schmiedmayer, and A. Zeilinger, *Phys. Rev. Lett.* **77**, 4980 (1996).
4. S. Bernet, M. K. Oberthaler, R. Abfalterer, J. Schmiedmayer, and A. Zeilinger, *Phys. Rev. Lett.* **77**, 5160 (1996).
5. (a) J. Fujita, M. Morinaga, T. Kishimoto, M. Yasuda, S. Matusi, and F. Shimizu, *Nature* **380**, 691 (1996); (b) M. Morinaga, M. Yasuda, T. Kishimoto, and F. Shimizu, *Phys. Rev. Lett.* **77**, 802 (1996).
6. D. O. Chudesnikov and V. P. Yakovlev, *Laser Phys.* **1**, 110 (1991).
7. H. Kogelnik, *Bell System Tech. J.* **48**, 2909 (1969).
8. R. J. Collier, C. B. Burckhardt, and L. H. Lin, *Optical Holography*, Academic Press (1971).
9. H. Batelaan, S. Bernet, M. K. Oberthaler, E. Rasel, J. Schmiedmayer, and A. Zeilinger, in *Atom Interferometry*, P. R. Berman, Ed., Academic Press, 1997.
10. (a) P. E. Moskowitz, P. L. Gould, S. R. Atlas, and D. E. Pritchard, *Phys. Rev. Lett.* **51**, 370 (1983); (b) P. L. Gould, G. A. Ruff, and D. E. Pritchard, *Phys. Rev. Lett.* **56**, 827 (1986).
11. P. J. Martin, B. G. Oldaker, A. K. Miklich, and D. E. Pritchard, *Phys. Rev. Lett.* **60**, 515 (1988).
12. D. M. Giltner, R. W. McGowan, and Siu Au Lee, *Phys. Rev. A*, **52**, 3966 (1995).
13. S. Dürr, S. Kunze, and G. Rempe, *Quant. Semiclass. Opt.* **8**, 531 (1996).

14. E. M. Rasel, M. K. Oberthaler, H. Batelaan, J. Schmiedmayer, and A. Zeilinger, *Phys. Rev. Lett.* **75**, 4598 (1995).
15. D. M. Giltner, R. W. McGowan, Siu Au Lee, *Phys. Rev. Lett.* **75**, 2638 (1995).
16. (a) B. W. Batterman, H. Cole, *Rev. Mod. Phys.* **36**, 681 (1964); (b) H. Rauch and D. Petrascheck in *Neutron Diffraction*, H. Dachs, Ed., Springer, p. 303, 1978.
17. M. A. Horne, K. D. Finkelstein, C. G. Shull, A. Zeilinger and H. J. Bernstein in *Matter Wave Interferometry*, p. 189, G. Badurek, H. Rauch, and A. Zeilinger, Eds., North Holland, 1988.
18. G. Borrmann, *Z. Physik*, **42**, 157 (1942).
19. S. Bernet, B. Kohler, A. Rebane, A. Renn, and U. P. Wild, *JOSA* **B9**, 987 (1992).
20. M. G. Friedel, *Comptes Rendus Acad. Sci. Paris* **157**, 1533–1536 (1913) (in French).
21. *International Tables for Crystallography Vol. A*, 3rd ed., Theo Hahn, Ed., Kluwer Academic Publishers, pp. 40 and 48, 1992.
22. C. Keller, R. Abfalterer, S. Bernet, M. K. Oberthaler, J. Schmiedmayer, and A. Zeilinger, submitted to *Phys. Rev. Lett.* (1997).
23. A. Steyerl, W. Drexel, S. S. Malik, and E. Gutsmedl, *Phys. B* **151**, 36, and references therein (1988). Neutrons were slowed by diffraction at moving sent through time-dependent potentials²⁴ or deflected by time-dependent mirrors.^{25,26} Recently, experiments have been performed with atomic matter waves^{27,28} where atoms released from a magneto-optical trap were reflected by a vibrating mirror.
24. G. Badurek, H. Rauch, and D. Tuppinger, *Phys. Rev. A* **34**, 2600 (1986).
25. R. Gaehler and R. Golub, *Z. Phys. B* **56**, 5 (1984).
26. J. Felber, R. Gähler, C. Rausch, and R. Golub, *Phys. Rev. A* **53**, 319 (1996).
27. A. Steane, P. Szriftgiser, P. Desibiolles, and J. Dalibard, *Phys. Rev. Lett.* **74**, 4972 (1995).
28. P. Szriftgiser, D. Guéry-Odelin, M. Arndt, and J. Dalibard, *Phys. Rev. Lett.* **77**, 4 (1996).
29. S. Bernet, M. K. Oberthaler, R. Abfalterer, J. Schmiedmayer, and A. Zeilinger, *Quantum Semiclass. Opt.* **8**, 497 (1996).
30. M. Moshinsky, *Phys. Rev.* **88**, 625 (1952).
31. A. S. Gerasimov, and M. V. Kazarnovskii, *Sov. Phys. JETP* **44**, 892 (1976).